Microfabrication by X-ray-Induced Polymerization Above the Lower Critical Solution Temperature

Vijay R. Tirumala,[1,2]* Gerard T. Caneba,[2] Derrick C. Mancini,[1] H. H. Wang[3]

[1]*Advanced Photon Source, Argonne National Laboratory, Argonne, Illinois 60439*
[2]*Department of Chemical Engineering, Michigan Technological University, Houghton, Michigan 49931*
[3]*Materials Science Division, Argonne National Laboratory, Argonne, Illinois 60439*

Received 17 August 2005; accepted 15 September 2005
DOI 10.1002/app.24073
Published online in Wiley InterScience (www.interscience.wiley.com).

ABSTRACT: A polymer synthesis method is presented in which chain growth driven by exothermic reaction stimulates a gradual chain collapse. The globular precipitates in such systems can be restrained from coalescing by polymerizing in a quiescent environment. Time-resolved small-angle scattering study of the methacrylic acid polymerization kinetics in a quiescent system above its lower critical solution temperature (LCST) in water reveals the following features of this method: (a) growing oligomers remain as rigid chains until a critical chain length is reached, at which they undergo chain collapse, (b) radius of gyration increases linearly with time until a critical conversion is reached, and (c) radius of gyration remains constant after the critical conversion, even while conversion is gradually increasing. Following this self-stabilizing growth mechanism, we show that nanoparticles can be directly synthesized by polymerizing *N*-isopropylacrylamide above its LCST in water. The average size of nanoparticles obtained from a polymer–solvent system is expected to be the maximum extent of reaction spread at that monomer concentration. This hypothesis was then verified by polymerizing *N*-isopropylacrylamide above their LCST in water, but by initiating the reaction with X-rays shielded by a mask. The microfabricated patterns conform well to the size and shape of the mask used confirming that the growing chains do not propagate beyond the exposed regions as long as the reaction temperature is maintained above the LCST. © 2006 Wiley Periodicals, Inc. J Appl Polym Sci 102: 429–435, 2006

Key words: hydrogels; polymerization; x-ray; scattering; lithography

INTRODUCTION

Free-radical polymerization reactions are typically unstable in nature due to the "run away" behavior associated with the uncontrolled and exothermic chain propagation reaction. Reaction control in free-radical polymerization, therefore, refers to regulating chain propagation. The so-called controlled polymerization chemistries[1–3] employ external chemical mediators (nitroxides, metal complexes, etc.) to regulate chain propagation, which in turn influences polydispersity and average molecular weight of the product. Most of these procedures, however, are not suitable to restrain the spatial extent of chain propagation and can only be used to produce polymers in bulk. Consequently, the synthesis of polymeric microstructures *in situ* requires the use of molds or multifunctional monomers along with photoinitiators.[4,5] The current study attempts to utilize an alternate reaction pathway that inherently stabilizes polymer chain growth, which, when combined with the principles of X-ray lithography, can be used to produce polymeric microstructures without the use of molds or specialty monomers.

Precipitation polymerization above the lower critical solution temperature (LCST)[6] uses the thermodynamic incompatibility between a solvent and a growing polymer chain to impart control over polymerization reaction. In this process, monomer is polymerized in a solvent that has the inverse-temperature-solubility environment (in other words, LCST) for the resulting polymer. Although not a living polymerization chemistry, such a process was shown to exert good control over product polymer properties and could be classified as a controlled polymerization with no chemical additives.[7,8] The reaction mechanism was proposed to rely on the coil-globule transition[9–13] of a polymer chain above the LCST to isolate the free-radical chain ends within precipitated globules. The trapped radicals can be activated later to react with a different monomer dissolved in a good solvent for the former polymer to produce block copolymers.[14,15] Phenomenological results from past researchers[7,8,14–16] support the proposed mechanism that coil-

Correspondence to: V. R. Tirumala (vijay@aps.anl.gov).
**Present address:* Polymers Division, National Institute of Standards and Technology, Gaithersburg, MD 20878.
Contract grant sponsor: U.S. Department of Energy, Office of Science, BES; contract grant number: W-31–109-Eng-38.
Contract grant sponsor: Michigan Tech Faculty Development Program.

to-globule transition plays a crucial role in controlling chain propagation, but it was not verified experimentally. We have previously used small-angle scattering to study the *in situ* growth kinetics, but the results were inconclusive probably because the system was sealed under vacuum instead of a nitrogen blanket. [17] Continuing our previous work, we show here that nanoparticles can be synthesized from *N*-isopropylacrylamide, which is well-known for its LCST in water.

The coil-globule transition phenomenon for polymers was well studied by several groups since Stockmeyer predicted it in 1960.[18] Most of the theoretical,[13,19–26] experimental,[27–38] and simulation[39–41] studies focused on polymer chain behavior below the upper critical solution temperature (UCST). It is evident from the literature that the coil-globule transition is continuous, but not instantaneous, and goes through intermediate states, such as a crumpled coil, before collapsing further into a compact globule at very high molecular weights. The phenomenon near the LCST, although similar, has not attracted the same attention until recently because the transition from a crumpled coil to a fully collapsed molten globule below the UCST itself is still not completely understood. Monte Carlo simulations of a polymer chain near the LCST showed that in the low-polymer-concentration region polymer chains exist in a crumpled coil conformation, while in the polymer-rich phase they exist in a more expanded state.[42] Laser light-scattering study has concluded[43] that a chain of monomers should be at least 10–20 random-steps long, before it can assume the properties of a polymer and behave like a Gaussian coil. By extending the same argument, it is apparent that a growing polymer chain above the LCST does not approach Gaussian statistics (nor does it feel the solvent quality) until it is long enough to be a polymer. Once the chain is long enough, solvent quality is felt forcing a change in its conformation gradually from an extended coil to a crumpled coil at intermediate molecular weights, and to a collapsed globule at very high molecular weights.

In the current study, we attempt to experimentally verify this hypothesis by time-resolved small-angle X-ray scattering of methacrylic acid polymerization, above its LCST in water. The experiment was setup to maintain a quiescent reaction environment in which forced interactions among polymer chains are minimized. From here on, we will call this a quiescent retrograde-precipitation, or QRP, environment. If our hypothesis were to be true, polymerization of reactive systems in the QRP region, when initiated with a highly collimated ionizing radiation, would also be limited only to the exposed regions even in the absence of multifunctional monomers or light-specific initiators. Ionizing radiation such as X-rays and gamma rays are conventionally known to produce free radicals from most organic species.[44–46] Direct ionization of species is occasionally prevalent, depending on the operating conditions and the systems under study.[47] For example, ionization of organic species is predominant at room temperature, while radical production is predominant at temperatures well above room temperature.[48] After radiation initiation of a system that is above the LCST of a growing polymer, control over chain propagation is expected to result in the confinement of growing polymer to the irradiated region.

EXPERIMENTAL

Materials used

Methacrylic acid (MAA) was purchased from Aldrich Chemical Company and was double distilled before use. *N*-isopropylacrylamide (99%+ pure) (NIPAm) was obtained from Arcos Organics and was used as obtained. The little amount of inhibitor present was assumed not to disrupt the reaction trajectory. Polymerization reaction initiators, VA-044 and V-50, were both purchased from Wako Chemical Company. The half-life of the initiators at the temperatures they were used (45°C and 80°C respectively) was 100 and 28 min, respectively.* Ethylene glycol dimethacrylate (EGDMA) and methylene bisacrylamide (BIS) were used as crosslinkers, where needed. Water was deionized before use, unless otherwise stated. All the solutions were degassed by bubbling nitrogen through, before subjecting them to reaction conditions.

Both the systems studied, poly (MAA) and poly (NIPAm), were chosen especially for their well-known phase transition behavior in water. The former has an LCST at 42°C[7] while the latter at 32°C.[49]

Time-resolved SAXS of MAA polymerization

Time-resolved small angle X-ray scattering was conducted at BESSRC beamline, 12-ID-C, of the Advanced Photon Source. MAA was polymerized in water at 80°C, which is clearly above the LCST. A MAA-water-soluble compound, V-50, was used as the reaction initiator. The reactive mixture was prepared by dissolving 12 g of MAA and 0.06 g of V-50 in 120 g of water. A quartz scattering tube was filled with a representative sample of this mixture and was capped with a cork to prevent solvent evaporation. A preliminary scan of the monomer mixture at room temperature was used as a background for correcting subsequent scattering data. Reaction was initiated (at time, $t = 0$) by placing the scattering tube in an in-house

*Wako product literature on azo-initiators.

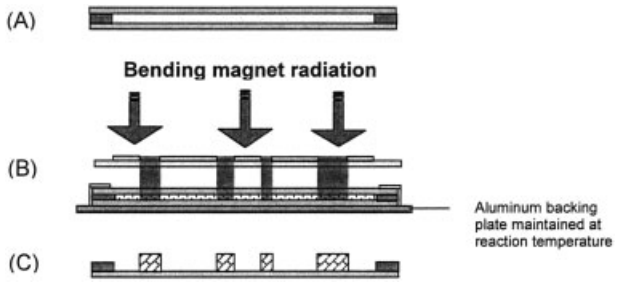

Figure 1 Experimental setup for Synchrotron-radiation-induced polymerization. (A) Monomer solution is captured between two silicon wafers separated by a spacer, (B) solution was maintained at a reaction temperature and exposed to X-rays through an X-ray mask, and (C) product polymer formed within the irradiated regions.

sample holder[50] maintained at 80°C. SAXS data was acquired every minute for 90 min.†

Polymerization in a quiescent environment

NIPAm was polymerized in a 1-mm-ID stainless steel tube reactor, which is assumed to maintain a quiescent fluid. A 0.08 g of NIPAm along with 0.3 mg of VA-044 was dissolved per 1 mL of water. EGDMA was added at 10% (wt/wt) to the monomer. The tube reactor was tightly sealed at one end, while the monomer solution was pumped in from the other end using an Eldex™ metering pump. Polymerization was carried out at 45°C, after which product from reactor was pumped out with water at same temperature and collected on a silicon wafer at liquid nitrogen temperature (−196°C). The solution was freeze-dried in slush (at −40°C) of mixed xylenes and liquid nitrogen and the product was imaged using atomic force microscopy (AFM).

Synchrotron-radiation-induced polymerization

A 20% (by weight) monomer solution was prepared by dissolving a mixture of NIPAm and BIS in water. BIS was added at 10 wt % with respect to the monomer. The mixture of monomers was also thoroughly degassed to prevent recombination of radical species with dissolved gases in the solvent.

Monomer solution was captured between two silicon wafers separated by a spacer and the wafer assembly was sealed first by using a Teflon-thread seal tape and then a Kapton tape. One of the wafer surfaces was oxidized to promote selective adhesion toward the resulting polymers. The sandwiched wafer system was mounted onto an aluminum backing plate, maintained at 45°C, in the path of the X-ray beam. This temperature is clearly above the LCST of poly (NIPAm) in water. The wafer assembly was exposed to the X-rays from a bending magnet at beamline 2-BM-B,[51] of the Advanced Photon Source.

An X-ray mask, prepared using photolithography and gold electroplating,[52] was used to spatially predefine the regions of exposure, as shown in Figure 1. After exposure, the wafer system was dismantled, and the product was air dried in a fume hood. Patterns were characterized by optical microscopy in a bright-field mode, using an Olympus BX-60 microscope.

RESULTS

TRSAXS of chain growth kinetics in a QRP environment

Figure 2 shows the reaction-induced change in scattering profile from the MAA polymerization at 80°C. The slope of scattering profiles changed from −1.5 at 2 min into the reaction, to −2 from about 10 min onwards. Following small-angle scattering from fractal systems,[53] it means that the polymer chain, with an increase in molecular weight, goes from a quasi-extended-chain conformation to a Gaussian coil. All the profiles were fit to the Debye function[54] since growing polymer chains, at least initially, were expected to be in ideal environment. Grosberg and Kuznetsov[21,22] have argued that polymer chains would again assume Gaussian chain conformation in the vicinity of the spinodal curve, justifying the use of Debye function to fit the scattering profiles through out the reaction. The radius of gyration of the growing polymer chains can be derived from the form factor, while the change in polymer concentration was assumed to result in a change in the intensity scale factor of the fit. The polymer chain growth kinetics were deduced by plotting both the radius of gyration and the scale factor as

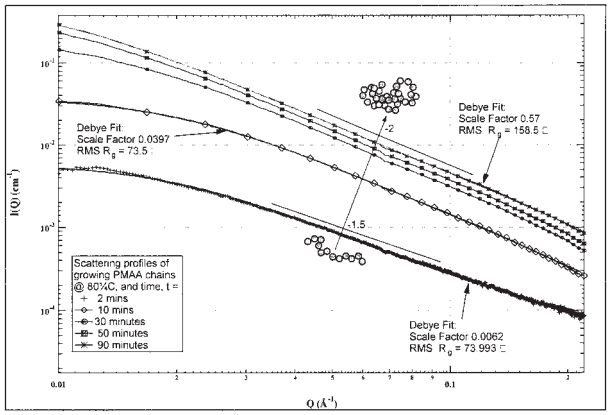

Figure 2 Time-resolved SAXS profiles of MAA polymerization in a QRP environment. Markers are experimental data and solid lines are model fits obtained for the Debye function.

†There was a 2-min time lag between the start of reaction and SAXS data acquisition.

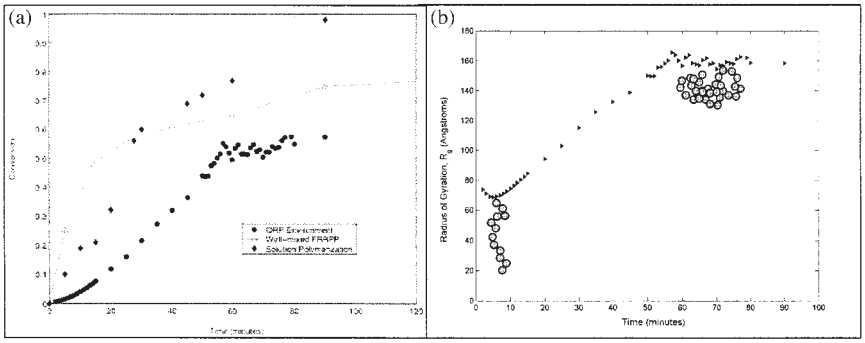

Figure 3 (a) Conversion profile of a quiescent retrograde-precipitation (QRP) system, compared with those of a well-mixed FRRPP system and a solution polymerization system[7] (left). (b) Chain growth profile of the QRP system in (a) (right).

a function of time, for the entire course of reaction (Fig. 3). As seen from Figure 3(a), the conversion in a QRP system gradually increased until two half-lives of the initiator before reaching a seemingly asymptotic conversion, about which it oscillates. A solution polymerization system undergoes a gel-effect condition to reach near 100% conversion. A well-mixed retrograde-precipitation system, on the other hand, undergoes an initial gel-effect but quickly controls the propagation reaction by means of phase separation and stabilizes well below complete conversion. The onset of decrease in conversion rate in a well-mixed system occurs at about one half-life of the initiator, while it gets delayed up to two half-lives in a quiescent environment. This also suggests that the chain growth in QRP systems is retarded due to limited availability of monomer within the collapsed globules.

The radius of gyration (R_g) profile shown in Figure 3(b) further illustrates the effect of chain collapse on reaction propagation. The R_g initially went through a minimum, unlike conversion, followed by a gradual increase and reached an asymptotic chain size at about the same time as that of the conversion. Monte Carlo simulations of polymer chain behavior in a retrograde phase envelope have shown that the mean end-to-end distance of a collapsed chain goes through a minimum near the LCST.[42] In that study, the simulations of a 20-mer, at constant pressure, showed a collapse from 35 Å to about 28 Å, in the vicinity of the LCST. Analogously, the minimum in the radius of gyration obtained from TRSAXS experiments corresponds to a critical chain length at which the average size of growing chains is long enough to behave like a polymer. Past that minimum, the collapse transition of the polymer chain resulted in a first-order increase in radius of gyration that later reached an asymptotic value at about two half-lives of the initiator (50 min). Note that the conversion steadily increases even as the radius of gyration has stabilized. Apart from the decreased propagation rates, this could be due partly to the rate of chain growth causing a proportional chain collapse, resulting in an oscillating R_g about the critical size of a globule. The rates of chain collapse and globular aggregation were found to depend on the temperature and molecular weight of the polymer in some recent studies.[36–38] They also observed that, below the UCST, an increase in temperature increases the rate of globular agglomeration.[38] In other words, the rate of globular agglomeration increases as the operating temperature nears the phase transition temperature. The phenomenon should be similar above the LCST too, in that the rate of globular agglomeration decreases with an increase in temperature. In precipitation polymerization above the LCST, operating temperature increases with an increase in polymer chain length (due to the exothermic reaction) and thereby decreases the rate of globular agglomeration. This also means that the polymer chains would not completely precipitate out of solvent, but instead continue to react slowly in the metastable region. The validation of this hypothesis was the reason behind polymerizing NIPAm in a QRP environment.

Quiescent fluid polymerization

Figure 4 shows a representative AFM micrograph of the freeze-dried poly (NIPAM-*co*-EGDMA) nanoparticles. Particle analysis of several such images, aver-

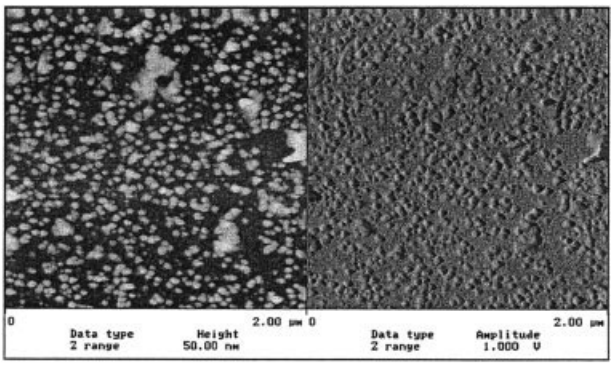

Figure 4 AFM topography scan of freeze-dried nanoparticles obtained from NIPAM-EGDMA polymerization in water. The left frame is based on height, while the right frame is based on amplitude.

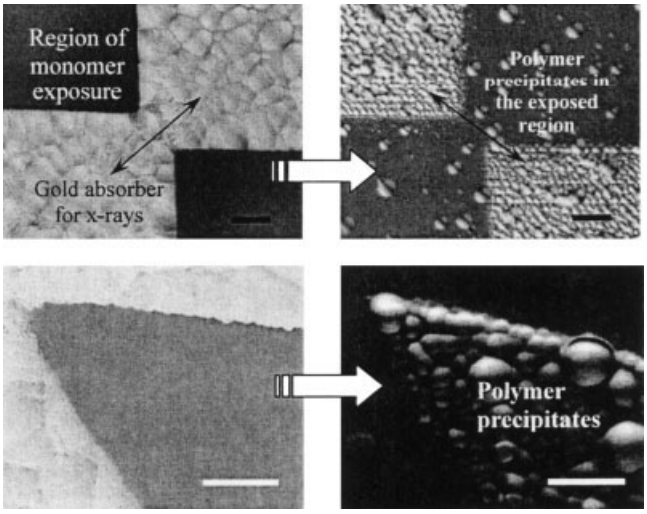

Figure 5 Optical micrographs of the poly (NIPAm-*co*-CaMe) pattern (right) produced as a result of the synchrotron-radiation-initiated QRP polymerization reaction through a mask (left). Note that the polymer precipitates limit themselves to the irradiated regions. Scale bar = 20 μm.

aged over 8000 particles (not presented here; using Nanoscope IIIa software from Digital Instruments, Inc.) indicated a mean end-to-end distance of 30–35 nm, by assuming a spherical shape for the particles. Styrene systems of our previous quiescent polymerization studies resulted in nanoparticles with no agglomeration.[17] In the case of NIPAm, however, some agglomeration was observed, which might be an after effect induced during the freeze-drying of aqueous solution.

In conventional polymerizing systems. NIPAm is polymerized below the LCST causing gelation to set in immediately, forming a bulk film. By polymerizing NIPAm in a QRP environment, gelation can be avoided to produce isolated globules in space. Unlike conventional vacuum drying, freeze-drying helps in keeping the globules unagglomerated. Because nanoparticles are precipitating from solution, their internal structure could be porous when swollen.[55]

Synchrotron-radiation-induced polymerization

It is apparent from both the time-resolved kinetic observations and synthesis of nanoparticles that chain growth is inherently stabilized in QRP polymerization systems. The controlled chain growth in such systems, when combined with the principles of lithography, offers a new paradigm in the fabrication of polymeric microstructures from the bottom-up, starting with a solution of monomers.

Spatioselective reaction initiation was achieved by irradiating the monomer solution with X-rays through a mask. Radiation initiation has the unique advantage of spatially uniform initiation reaction, unlike a more statistically distributed random chemical initiation. If chain propagation were to remain uncontrolled even under QRP conditions, the resulting polymer from radiation initiation through a mask should be nonconforming to the shape of the mask. The spatial propagation aspects of the process could, therefore, be verified by polymerizing the monomer in the presence of a crosslinker with low reactivity with the monomer. Such a crosslinker will not readily crosslink the material, thus allowing the monomer to propagate freely. Calcium methacrylate (CaMe, prepared by neutralizing calcium hydroxide with methacrylic acid) was, therefore, used to check the validity of the proposed hypothesis and also the extent of chain propagation in QRP systems. Unlike free radical crosslinkers, such as bisacrylamide, calcium methacrylate would ionize upon irradiation and would not react with the free-radical chain ends of NIPAm. Figure 5 shows a poly (NIPAm-*co*-CaMe) pattern produced as a result of spatially defined radiation initiation. The thickness of the patterns does not exceed beyond a micron for irradiation times in the range of 10–15 min, which is another evidence of the low reactivity of CaMe. Methylene bisacrylamide (BIS), on the other hand, rapidly crosslinks even 500-μm-thick monomer solutions in a few minutes of exposure. As seen from the figures, the polymer pattern matches the X-ray mask well. The unexposed regions still show some polymer particles that are less significant compared to that of the irradiated regions.

First results from the poly (NIPAm-*co*-BIS) based microgel synthesis are also presented here. Fourier transform infrared spectroscopy characterization of the absorption bands revealed no impurities in the product polymer. The transmission spectrum also matches well with that of the same polymer prepared by chemical synthesis. Figure 6 shows a 100-μm-wide line pattern of poly (NIPAm-*co*-BIS) in a dry state and in a swollen state. The extent of crosslinking is evident from the swelling exhibited by the patterns when wetted. Gels prepared from this synchrotron-radiation-

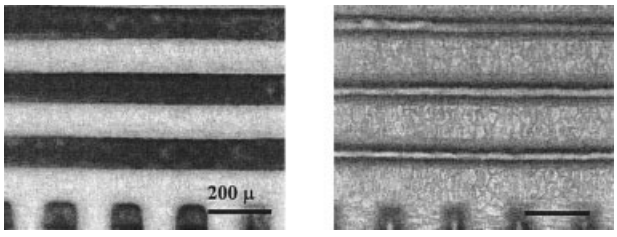

Figure 6 Poly (NIPAm-*co*-BIS) pattern produced via synchrotron-radiation-induced polymerization in a QRP environment: in a dry state (left) and a swollen state (right).

induced polymerization were found to retain their reversible swelling behavior.[56] Gel response to a change in hydration or temperature was also found to be fast due to their unique pattern-dependant morphology.[57]

DISCUSSION

The difference in conversion-time profiles of the three polymerization environments compared in Figure 2 can be explained by considering the polymer chain behavior during the course of reaction. At the start of the reaction, growing oligomers would not feel the effect of solvent and would remain in solution as rigid chains. In solution polymerization, the growing polymer chains interact freely with the solvent and continue to react with the dissolved monomers to reach 100% conversion. In well-mixed precipitation polymerization above the LCST too, chain propagation would not be suppressed until the molecular weight of the polymer is high enough to be affected by the phase envelope. It is, therefore, characteristic of such systems to show an initial rapid change in conversion and asymptotically reach a final value that is well below 100%.6–8,16,17 The conversion-time profile of a well-mixed precipitation polymerization above the LCST shown in Figure 3(a) clearly shows two distinct growth regimes: (i) a rapid conversion rate in solution and (ii) suppressed rates due probably to precipitation. Before the critical conversion corresponding to precipitation, polymerization reaction rate would be rapid due to high reaction temperature. Beyond a critical molecular weight, chain collapse to crumpled coils occurs but reaction might still proceed at a relatively high rate since the free-radical chain ends can still react with dissolved monomers from solvent. Only after the reaction proceeds to very high molecular weights that collapse to molten globules can occur. Wu and Wang, however, have shown that 66% of the hydrodynamic molten globule volume is still filled with solvent.[58] This negates the mechanism put forth for the synthesis of block copolymers from precipitation polymerization above the LCST. In precipitation polymerization above the LSCT, conversion rate at the start of the reaction is much slower than in solution or well-mixed systems. We believe that this is due to the lack of widespread interactions among growing polymer chains. Chain propagation reaction would, therefore, be diffusion-controlled from the beginning of reaction in quiescent precipitation polymerization systems above the LCST. The continued reaction within these quasi-precipitates would eventually place the system near the spinodal curve, at which mutual diffusivities vanish. In the absence of mutual diffusivity, polymerization reaction continues only until it exhausts all the available monomer within the quasi-precipitates. Polymerization reaction rates beyond this time would be significantly lower. The system as a whole might still not show significant precipitation since precipitates remain unagglomerated. The oscillations observed in both conversion and radius of gyration (Fig. 3), at the end of the reaction, are consistent with the hypothesized behavior of a growing polymer chain in the vicinity of spinodal curve above the LCST.

The stabilized chain growth phenomenon in a QRP environment is caused by the thermodynamic interplay between exothermic reaction and retrograde-precipitation. Therefore, polymer chain propagation should remain well controlled irrespective of the initiation method. In radiation-induced polymerization, we believe that the chain growth is similarly stabilized and continued irradiation causes the precipitated polymer globules to further react with each other and form a micropattern. This was also supported by the poly (NIPAm-*co*-CaMe) patterns, which appear to be an assembly of polymeric precipitates. The patterns of irradiation were clearly demarcated by the globules lining up along the edge. This could be due to the lower crosslinking activity of calcium methacrylate because, for the same irradiation time, patterns already assume bulk microscopic structure when BIS is used. We found that the spatially limited chain growth is unique only to systems polymerized in a QRP environment. For example, NIPAm when polymerized below the LCST in solution resulted only in a bulk film with reliefs of irradiated patterns on its surface.

CONCLUSIONS

Polymerization in a retrograde-precipitation environment belongs to the class of controlled synthesis that does not involve the use of chemical mediators. In well-mixed systems, chain termination was found to be diffusion-controlled throughout the reaction while propagation was found to be diffusion-controlled only after precipitation. In a quiescent precipitation environment above the LCST, we believe that both chain termination and propagation become diffusion-controlled right from the initial stages of polymerization. The reaction in a QRP environment is thus self-stabilizing, leading to the formation of isolated nanoparticles. When polymerization in a quiescent inverse-precipitation environment is instead initiated with ionizing radiation, diffusion-controlled chain propagation limits the chain growth only to the irradiated regions. Moving away from the conventional molding and micromachining of polymers, this offers a unique reaction pathway for the synthesis of soft-matter-based micro- and nanostructures. The spatial resolution of this radiation-induced polymerization is believed to be the average size of the nanoparticles, which is the smallest precipitate formed from a conventional chemical initiation system. The technique presented here can be used in the high through-put microfabrication of scaffolds for cell grafting and tissue engineering.[59]

References

1. Wang, J.-S.; Matyjaszewski, K. Macromolecules 1995, 28, 7901.
2. Georges, M. K.; Veregin, R. P. N.; Kazmaier, P. M.; Hamer, G. K. Macromolecules 1993, 26, 2987.
3. Davis, T. P.; Haddleton, D. M.; Richards, S. N. J Macromol Sci—Rev Macromol Chem Phys C 1994, 34, 243.
4. Gozzelino, G.; Liturri, S.; Audisio, G. Nucl Instrum Methods B, 2001, 185, 248.
5. Terrones, G.; Pearlstein, A. J. Macromolecules 2001, 34, 3195.
6. Caneba, G. T. Adv Polym Tech 1992, 11, 277.
7. Aggarwal, A.; Saxena, R.; Wang, B.; Caneba, G. T. J Appl Polym Sci 1996, 62, 2039.
8. Wang, B.; Dar, Y. L.; Shi, L.; Caneba, G. T. J Appl Polym Sci 1999, 71, 761.
9. Nierlich, M.; Cotton, J. P.; Farnoux, B. J Chem Phy 1978, 69, 1379.
10. Sanchez, I. C. Macromolecules 1979, 12, 980.
11. Nishio, I.; Swislow, G.; Sun, S.; Tanaka, T. Nature 1982, 300, 243.
12. Kholodenko, A. L.; Freed, K. F. J Phy A: Math Gen 1984, 17, 2703.
13. Raos, G.; Allegra, G. J Chem Phy 1996, 104, 1626.
14. Caneba, G. T.; Dar, Y. L. U.S. Pat. Appl. 20,030,153,708 (2003).
15. Caneba, G. T.; Zhao, Y.; Dar, Y. L. J Appl Polym Sci 2003, 89, 426.
16. Dar, Y.; Caneba, G. T. Chem Eng Commun 2002, 189, 571.
17. Tirumala, V. R.; Caneba, G. T.; Dar, Y. L.; Wang, H. H.; Mancini, D. C. Adv Polym Tech 2003, 22, 126.
18. Stockmeyer, W. H. Makromol Chem 1960, 35, 54.
19. de Gennes, P. G. J Phys Lett 1975, 36, L55.
20. Lifshitz, I. M.; Grosberg, A. Y.; Khokhlov, A. R. Rev Mod Phys 1978, 50, 683.
21. Grosberg, A. Y.; Kuznetsov, D. V. Macromolecules 1992, 25, 1970: a series of three papers;
22. Grosberg, A. Y., Kuznestov, D. V. Macromolecules 1993, 26, 4249.
23. Sanchez, I. C., Macromolecules 1979, 12, 980.
24. Raos, G.; Allegra, G. Macromolecules 1996, 29, 6663.
25. Raos, G.; Allegra, G. Macromolecules 1996, 29, 8565.
26. Raos, G.; Allegra, G. J Chem Phy 1997, 107, 6479.
27. Sun, S. T.; Nishio, I.; Swislow, G.; Tanaka, T. J Chem Phys 1980, 73, 5971.
28. Swislow, G.; Sun, S. T.; Nishio, I.; Tanaka, T. Phys Rev Lett 1980, 44, 796.
29. Park, I. H.; Wang, Q.-W.; Chu, B. Macromolecules 1987, 20, 1965.
30. Chu, B.; Park, I. H.; Wang, Q. W.; Wu, C. Macromolecules 1987, 20, 2833.
31. Chu, B.; Xu, R. L.; Zuo, J. Macromolecules 1988, 21, 273.
32. Chu, B.; Xu, R.; Wang, Z.; Zuo, J. J Appl Cryst 1988, 21, 707.
33. Chu, B.; Ying, Q.; Grosberg, A. Y. Macromolecules 1995, 28, 180.
34. Wu, C.; Zhou, S. Macromolecules 1995, 28, 8381.
35. Wang, X., Qiu, X., Wu, C. Macromolecules 1998, 31, 2972.
36. Nakata, M Phys Rev E 1995, 51, 5770.
37. Nakata, M.; Nakagawa, T. Phys. Rev. E 1997, 56, 3338.
38. Nakamura, Y.; Sasaki, N.; Nakata, M. Macromolecules 2001, 34, 5992 and the references therein.
39. Sotta, P.; Lesne, A.; Victor, J M. J Chem Phys 2000, 112, 1565.
40. Sotta, P., Lesne, A.; Victor, J. M. J Chem Phys 2000, 113, 6966.
41. Kuznetsov, Y. A.; Timoshenko, E. G.; Dawson, K. A. J Chem Phys 1996, 104, 3338 and the references therein.
42. Luna-Barcenas, G.; Gromov, D. G.; Meredith. J. C.; Sanchez, I. C.; de Pablo, J. J.; Johnston, K. P. Chem Phys Lett 1997, 278, 302.
43. Ding, Y.; Kisliuk, A.; Sokolov, A. P. Macromolecules 2004, 37, 161.
44. Chapiro, A. Radiation Chemistry of Polymeric Systems; Interscience Publishers: Great Britain, 1962.
45. Grosmangin, J.; Magat, M. Chem Commun 1957, 22, 141.
46. Burnett, G. M. Mechanisms of Polymerization Reaction, Interscience Publishers: New York, 1954.
47. Westlake, J. F.; Huang, R. J Polym Sci Part A-1: Polym Chem 1972, 10, 1429.
48. Moore, P. W.; Clouston, J. G.; Chaplin, R. P. J Polym Sci Polym Chem Ed 1983, 21, 2491.
49. Schild, H. G.; Muthukumar, M.; Tirrel, D. A. Macromolecules 1991, 24, 948.
50. Hessler, J. P.; Seifert, S.; Winans, R. E.; Fletcher, T. H.. Faraday Discussions 2001, 119, 395.
51. Lai, B.; Mancini, D. C.; Yun, W.; Gluskin, E. Proc. SPIE 1996, 2880, 171.
52. Mancini, D. C.; Moldovan, N. A.; Divan, R.; DeCarlo, F.; Yaeger. J Proc SPIE 2001, 4557, 77.
53. Teixeira, J. J Appl Cryst 1988, 21, 781.